ISSN 1068-3755, Surface Engineering and Applied Electrochemistry, 2020, Vol. 56, No. 4, pp. 415–426. © Allerton Press, Inc., 2020.
Russian Text © The Author(s), 2020, published in Elektronnaya Obrabotka Materialov, 2020, No. 4, pp. 10–20.

Validated Electrochemical Method for Simultaneous Resolution of Tyrosine, Uric Acid, and Ascorbic Acid at Polymer Modified Nano-Composite Paste Electrode

Chenthattil Raril[a], Jamballi G. Manjunatha[a,*], Doddarasinakere K. Ravishankar[b], Santosh Fattepur[c], Gurumallappa Siddaraju[d], and Lingappa Nanjundaswamy[e]

[a] *Department of Chemistry, FMKMC College, Madikeri, Mangalore University Constituent College, Karnataka, 571201 India*
[b] *Department of Chemistry, Sri Mahadeshwara Goverment First Grade College, Kollegal, Chamarajanagar, Karnataka, 571440 India*
[c] *School of Pharmacy, Management and Science University, @ Malaysia*
[d] *Department of Chemistry, JSS College for women Chamarajanagar, Karnataka, 571313 India*
[e] *UGC – Human Resource Development Centre, University of Mysore, Manasagangotri, Karnataka, Mysore, 570006 India*
**e-mail: manju1853@gmail.com*

Received October 28, 2019; revised November 11, 2019; accepted November 18, 2019

Abstract—In this work, an electrochemical sensor based on a poly threonine modified graphite-carbon nanotube paste electrode was developed for the investigation of tyrosine. The modification of the electrode was characterized by field emission scanning electron microscopy, cyclic voltammetry, and differential pulse voltammetry. The modified electrode shows many advantages such as simple preparation, good sensitivity, short response time, good stability and reproducibility. The developed electrode was highly selective because of the determination of tyrosine in the presence of the ascorbic acid and the uric acid. Under optimal conditions; the cyclic voltammetry provides a linear response with the concentration range from 2×10^{-6} to 2.5×10^{-5} M and 3×10^{-5} to 1.2×10^{-4} M with the limit of detection and limit of quantification values of 2.9×10^{-7} and 9.6×10^{-7} M. The developed sensor was employed for tyrosine detection in pharmaceutical sample, recoveries obtained were in a range of 99.0 to 102.80%.

Keywords: tyrosine, carbon nanotube, cyclic voltammetry, graphite powder, biosensor

DOI: 10.3103/S1068375520040134

INTRODUCTION

Tyrosine (Tyr) is an essential aromatic amino acid precursor for thyroxine, dopamine, adrenalin, and noradrenalin [1]. As reported elsewhere, high Tyr containing foods such as cheese, eggs, dairy, and beans could improve people's memory when under stress [2]. Hypochondrium, depression, and some other psychological diseases can be results of the deficiency of Tyr [3]. Therefore, it becomes a paramount task to develop an efficient analytical method for the resolution of Tyr in nutriment samples. The uric acid (UA) is a major nitrogenous compound in urine. The concentration of UA is around 2 mM in urine and 120 to 450 mM in the blood of healthy persons. Normally, healthy human beings excrete 400 to 700 mg urine per day. The abnormal UA levels reveal such problems as gout, hyperuricemia, or Lessch-Nyhan syndrome. Ascorbic acid (AA) is a water-soluble vitamin that is found in biological systems and foodstuffs; it acts as strong antioxidant [4]. The surplus of amino acids can lead to gastric irritation. Various analytical techniques have been reported elsewhere for the resolution of Tyr, such as chemiluminescence chromatography, spectrophotometry, and capillary electrophoresis [5–9]. Those methods are time-consuming and expensive, they also have low sensitivity in the determination of Tyr. To conquer these defects, electrochemical methods are extensively used due to their good sensitivity, reproducibility, and low cost.

For the past few decades, chemically modified electrodes became the focus of interest of researchers due to their potential application in a variety of analyses [10–27]. Carbon nanotubes (CNTs) and graphite carbon electrodes have got considerable attention due to their extraordinary advantages over conventional electrodes such as an improved mass transport, high porosity, a highly effective surface area, and reactive sites; they also provide a feasible platform for electroanalysis. In the past few years, carbon electrodes were applied and described for the fabrication of electrochemical sensors and biosensors [28–36]. Among a wide variety of modification results are, the amino

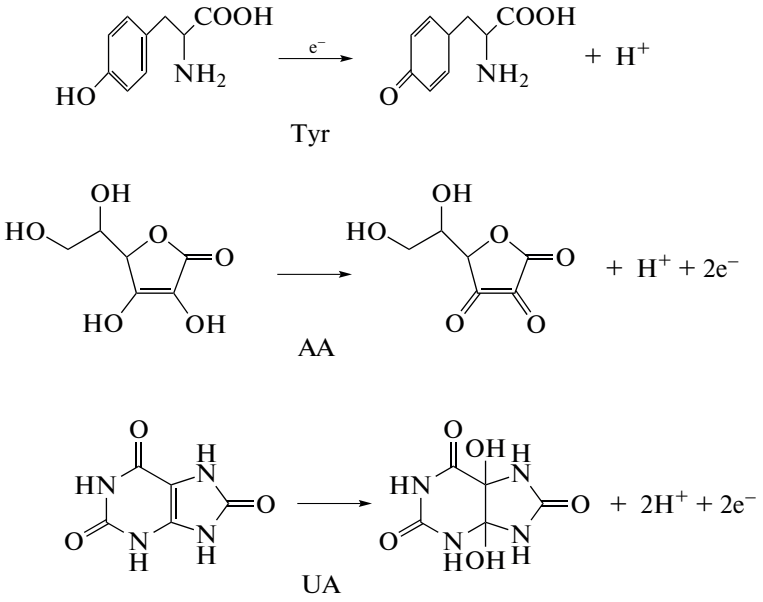

Fig. 1. Schemes of oxidation mechanisms of Tyr, AA, and UA.

acid modified electrodes that have lots of advantages like biocompatibility, stability, easy availability. Electropolymerization is extensively used for the preparation of polymer-modified electrodes by adjusting electrochemical parameters, which can control the film thickness (a polymer film shows excellent stability and reproducibility) and charge transport characteristics.

This study deals with the electrochemical investigation of Tyr at a mixed carbon paste electrode made from graphite powder and carbon nanotubes modified by threonine (Thr) by electro-polymerization. The method is based on subduing the peak current of the modifier due to the analyte in a modified carbon paste electrode. Compared to the oxidation response of a bare graphite-carbon nanotube paste electrode (BGCNT/PE) that at the modified electrode was remarkably higher. In addition, a simultaneous study of UA and AA was also carried out. The developed modified electrode was employed for the resolution of Tyr in real sample. The oxidation mechanism of Tyr, UA, and AA are schematically presented in Fig. 1.

EXPERIMENTAL

Chemicals and Reagents

Both Tyr and Thr were uses as obtained from Molychem. Graphite, silicone oil, and KCl were used as procured from Nice Chemical Pvt. Ltd. CNTs purchased from Sisco Research Laboratories Pvt. Ltd. Mumbai. Di-hydrogen sodium phosphate, di-sodium hydrogen phosphates, and $K_4[Fe(CN)_6]$ were used as procured from Merck. The Thr (25×10^{-3} M) and Tyr (25×10^{-4} M) stock solutions were prepared using a suitable solvent (diluted HCl). A 0.1 M phosphate buffer solution (PBS), as a supporting electrolyte, was made by combining a suitable amount of monosodium di-hydrogen phosphate and di-sodium hydrogen phosphate.

Instrumentation

Electrochemical measurements were made with a potentiostat CHI6038 E. All experiments were carried out with a conventional three-electrode cell that consisted of a platinum wire as auxiliary electrode, (BGCNT/PE) and poly threonine modified graphite-carbon nanotube paste electrode (PT/GCNT/PE) as working electrode and calomel electrode as reference electrodes. The prepared electrodes such as BGCNT/PE and PT/GCNT/PE was characterized by field emission scanning electron microscopy (FESEM) with a device from DST-PURSE Laboratory, Mangalore University.

Development of Bare Graphite-Carbon Nanotube Paste Electrode

The BGCNT/PE was developed by combining graphite (35%), CNTs (35%), and silicone oil (30%) in an agate mortar for 20 minutes for homogeneous paste. The prepared paste was tightly packed into a cavity (3 mm) of the electrode, and then the surface was polished by tissue paper.

RESULTS AND DISCUSSION

Electropolymerization of Threonine on Bare Graphite-Carbon Nanotube Paste Electrode

The electrochemical polymerization technique was used for the preparation of PT/GCNT/PE in 0.1 M

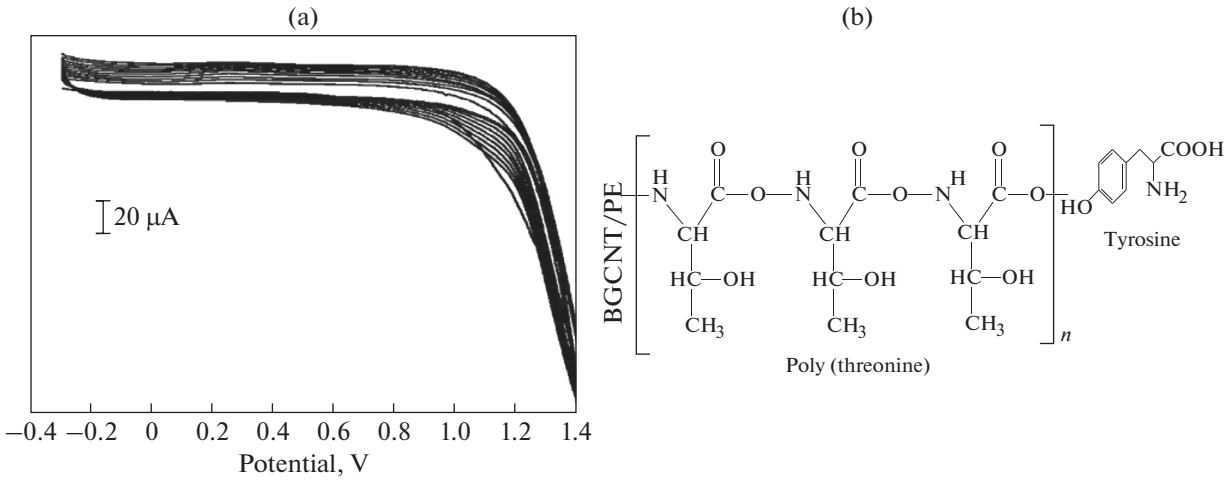

Fig. 2. (a) CVs for electropolymerization of 1×10^{-3} M of Thr on BGNT/PE in 0.1 M PBS, pH 7.0, scan rate – 0.1 V/s; and (b) Proposed polymerization structure of Thr at the surface of BGCNT/PE.

PBS (pH 7.0) containing 1×10^{-3} M of Thr at the potential window from –0.3 V to 1.4 V at a scan rate of 0.1 V/s (Fig. 2a). The peak current increased with an increased number of cycles; thus a polymeric film was grown on the surface of the bare electrode. The current response was maximum for 10 cycles, after that it decreased. Hence 10 cycles were chosen as the most favorable scan number. After 10 cycles, the exterior of the modified electrode was rinsed with distilled water to remove the physically adsorbed material. The suggested polymerization structure of threonine on BGCNT/PE is shown in Fig. 2b.

Cyclic Voltammetric Iinvestigations

To study the electrochemical behaviour of the bare and the modified electrodes, 1 mM $K_4[Fe(CN)_6]$ and KCl solution with a sweep rate of 0.1 V/s were chosen. Figure 3a shows the cyclic voltammetric behaviour of $K_4[Fe(CN)_6]$ at PT/GCNT/PE (curve *a*) and BGCNT/PE (curve *b*). It is evident that the anodic and cathodic peaks increased due to modification but ΔE_p became lower at the modified electrode (BGCNT/PE = 0.163 V, PT/GCNT/PE = 0.077 V). This result shows that the electron transfer process and electroanalytical activities have been highly improved at the modified electrode.

Figure 3b displays the cyclic voltammogram of 1 mM $K_4[Fe(CN)_6]$ with various scan rates from 0.1 to 0.250 V/s, at PT/GCNT/PE. It was noticed that the peak current increased at a higher scan rate. The oxidation peak current on the scan rate shows the linear response with the linear regression equation of I_{pa} (μA) = 7.43 + 149.87*v* (V/s) with the correlation coefficient of 0.99. Figure 3c shows the CVs of the bare electrode for different scan rates. It was observed that the peak current increased linearly with an increase of the scan rate, with the regression equation of I_{pa} (μA) = 7.69 + 25.95*v* (V/s), with the correlation coefficient of 0.99. The peak current response is related to the square root of the scan rate according to the following equation, [37]

$$I_p = Kn^{3/2}AD^{1/2}Cv^{1/2}, \quad (1)$$

where I_p is peak current, the constant K is 2.69×10^5; n is the number of electrons transferred per mole of electroactive species; A is the active surface area of the electrode in cm^2; D is the diffusion coefficient (6.70×10^{-6} cm^2/s); C is the concentration in mol/L (1 mM); and v is the scan rate of the potential in V/s. From the slope of the plot I_p vs $v^{1/2}$ of the bare and modified electrodes, the surface area, as calculated from the above equation, was found to be equal to 0.0325 and 0.1613 cm^2 for the bare and modified electrodes, respectively. This indicates that the BGCNT/PE when modified with Thr by electro-polymerization significantly increases the surface area of the working electrode.

Morphological Studies

Morphological behaviour of the bare and modified electrodes was characterized by FESEM. Fig. 4a shows the FESEM image of BGCNT/PE, with an irregularly arranged structure. Fig. 4b is the FESEM image of PT/GCNT/PE. It demonstrates that the bare electrode was subject to electro-polymerization of Thr, with a uniform film of the latter being deposited on the surface of the former.

Electrochemical Behaviour of Tyrosine

To evaluate the electrochemical properties of Tyr, both the modified and the bare electrodes were stud-

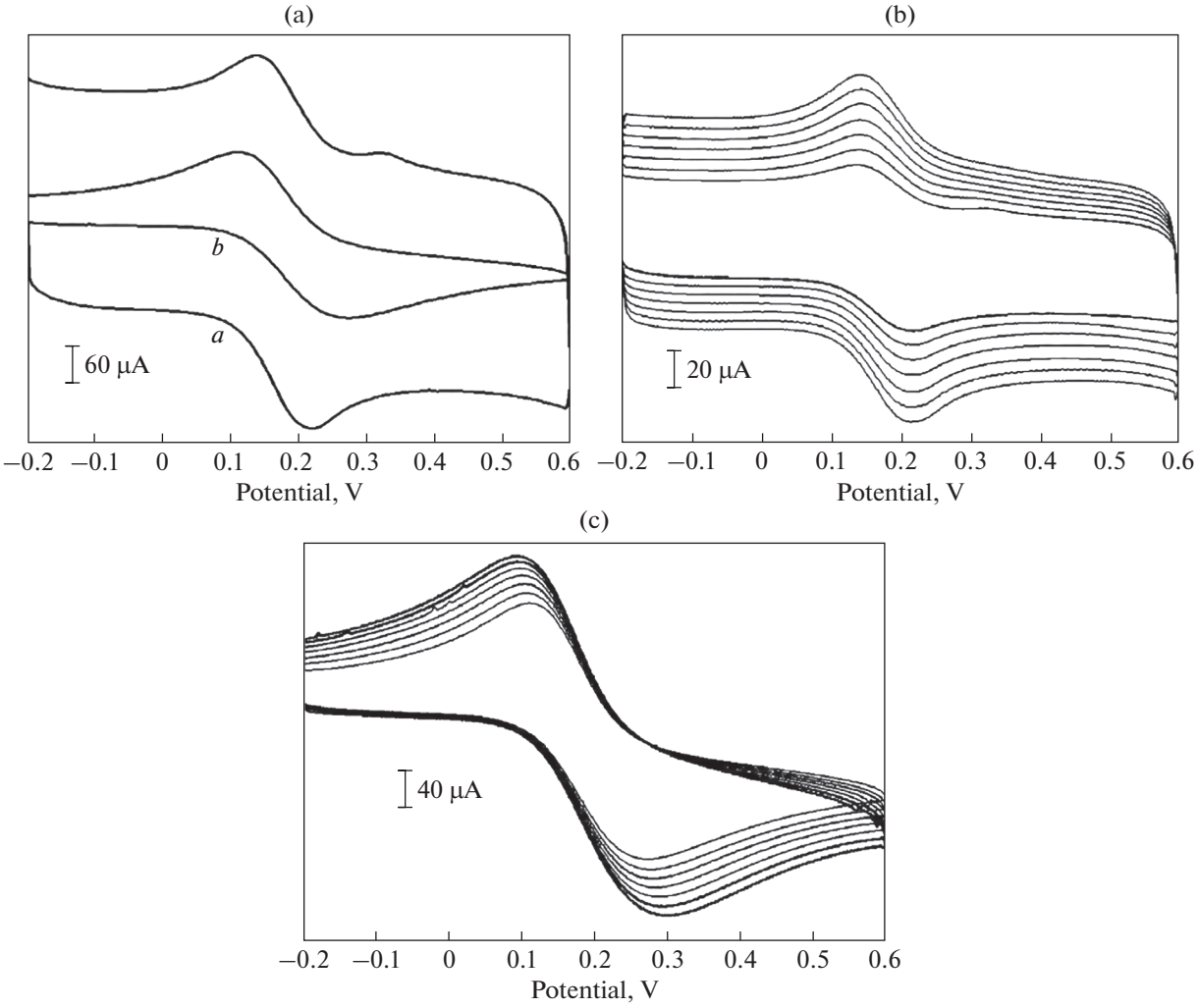

Fig. 3. (a) CVs of 1 mM $K_4[Fe(CN)_6]$ at PT/GCNT/PE (curve *a*) and BGCNT/PE (curve *b*) in 1 M KCl; (b) CVs of 1 mM $K_4[Fe(CN)_6]$ at PT/GCNT/PE in 1 M KCl with different scan rates (0.1 to 0.250 V/s) and (c) CVs of 1 mM $K_4[Fe(CN)_6]$ at BGCNT/PE in 1 M KCl with different scan rates.

ied in 0.1 M PBS (6.5 pH) containing 1×10^{-4} M Tyr, at a scan rate of 0.1 V/s (Fig. 5). An electro-catalytic reaction at the electrode surface runs usually via the exchange of protons with the solution. As can be seen, the modified electrode (curve *a*) has a higher peak current than that of the bare electrode (curve *b*), with a peak current of 21.48 μA and its potential of about 0.604 V. It confirms the fact that the presence of a polymer film at the electrode surface can contribute to the sensitivity of the developed sensor.

Figure 6 shows the CVs of the blank solution and of the solution containing electroactive species at the modified electrode (curve *a*), with a scan rate of 0.1 V/s in 0.1 M PBS of pH 6.5. As can be seen, no oxidation peak was noticed for the blank solution (curve *b*) but upon the addition of Tyr into the solution, an anodic peak was observed at the potential of 0.604 V, with the current response of 21.48 μA. It means that the admirable catalytic activity of the polymer film can also play an essential role in the electrooxidation of Tyr at the surface of the modified electrode.

Effect of pH on Oxidation of Tyrosine

The oxidation of Tyr is evidently affected by pH. The oxidation peak current and the oxidation potential of Tyr were investigated in a pH range of 6.0–8.0, in 0.1 M PBS, with the sweep rate of 0.1 V/s. Figure 7a shows the CVs of Tyr at various pH values. It can be observed that an a higher pH, the oxidation peak potential for Tyr shifts to negative values because a pH increase indicated that there was a proton, at least, involved in the oxidation reaction; the maximum current was obtained at pH 6.5 (Fig. 7b). The pH and E_{pa} relationship was linear, and a regression equation was: E_{pa} (V) = 0.967–0.0564 pH (Fig. 7c), with the coefficient of correlation 0.983. The value of 0.056 V/pH (slope) indicates that the electrode obeys the Nernst

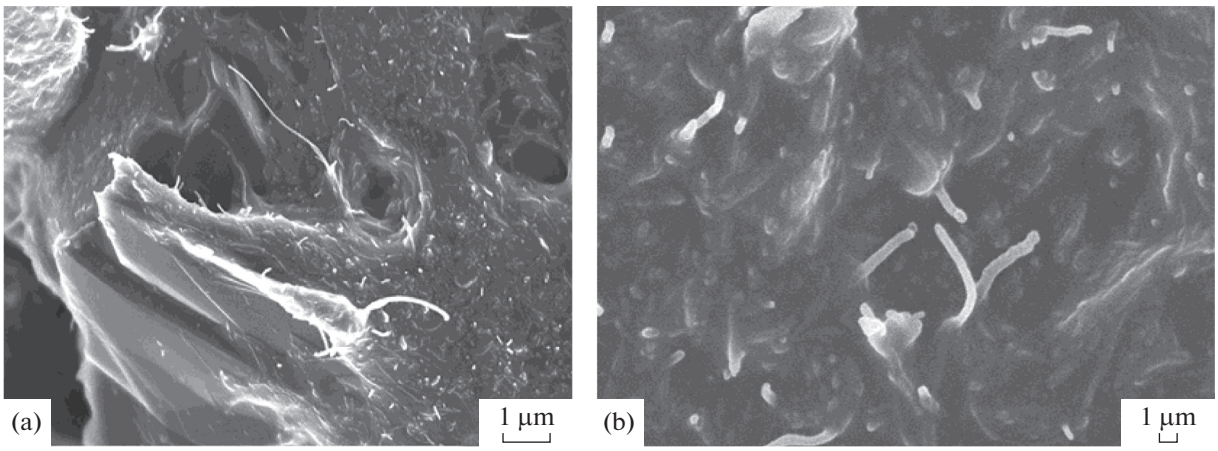

Fig. 4. FESEM images of: (a) BGCNT/PE, and (b) PT/GCNT/PE.

equation that involves the proton and the electron in a 1:1 (*m/n*) ratio [38–40]. The mechanism is in accordance with Tyr scheme presented in Fig. 1. The proton transfer number (*m*) is equal to the electron transfer number (*n*).

Effect of Sweep Rate

The relationship between the sweep rate and the peak current can give useful information on the electrochemical mechanism. Figure 8a shows the impact of the sweep rate on the oxidation peak current. According to Fig. 8b, the anodic peak current was amplified linearly, with the scan rate in a range of 0.1–0.275 V/s, with the linear regression equation of I_{pa} (μA) = 9.92 + 84.63*v* (V/s), with the correlation coefficient of 0.99, which confirms the adsorption controlled process [41, 42], at the electrooxidation of Tyr at the surface of the modified electrode. The relation between the peak potential and the log of the scan rate is as follows (Fig. 8c) [43],

$$E_{\mathrm{p}}(V) = \left[\frac{2.303RT}{2(1-\alpha)nF}\right]\log(v) + K, \qquad (2)$$

where *R*, *T*, and *F* are the gas constant, the temperature, and the Faraday constant, respectively; α is the electron transfer coefficient; and *n* is the number of electrons involved in the reaction. The slope $2.303RT/2(1-\alpha)\,nF$ is equal to 0.05817; the α value was assumed to be 0.5 (irreversible process). Based on the above equation, the number of electrons was calculated to be 1.016, which was close to the ideal value.

Effect of Variation of Concentrations

To evaluate the correlation between the oxidation peak current and the concentration of Tyr, the CV experiment was executed with diverse concentrations

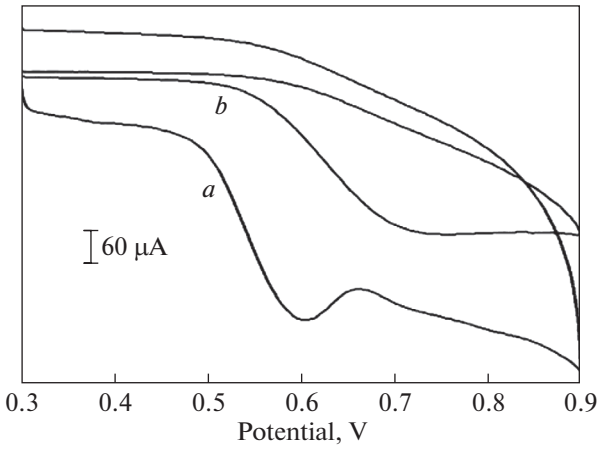

Fig. 5. CVs of 1×10^{-4} M Tyr at PT/GCNT/PE (curve *a*) and BGCNT/PE (curve *b*) in 0.1 M PBS, pH 6.5, scan rate – 0.1 V/s.

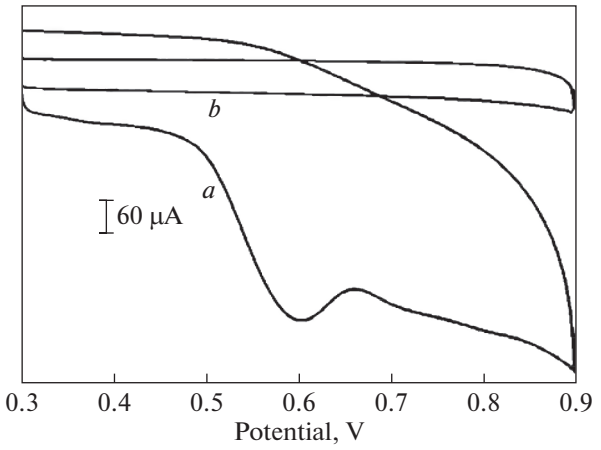

Fig. 6. CVs of 1×10^{-4} M Tyr at PT/GCNT/PE (curve *a*) and for blank solution (curve *b*) in 0.1 M PBS, pH 6.5, scan rate – 0.1 V/s.

Table 1. Comparison of detection limits of the proposed method with those reported elsewhere

Modified electrode	Technique	Linear range, μM	Detection limit, M	Reference
Graphene nanosheet/GCE	DPV	5.0–120.0	2.0×10^{-8}	[46]
ERGO/GCE	DPV	0.5–80.0	0.2×10^{-6}	[47]
CNF/ CPE	CV	0.2–107.0	0.1×10^{-6}	[48]
SDS/CNTPE	CV	2.0–50	7.29×10^{-6}	[49]
CPE-CNT/SDS	DPV	3.6–240.0	1×10^{-7}	[50]
PT/CPE	DPV	0.5 to 10 and 10 to 250	1×10^{-8}	[51]
		2.0 to 25 and 3.0 to 120		
PT/GCNT/PE	CV		2.9×10^{-7}	Present work

GCE: glassy carbon electrode; ERGO: electrochemically reduced graphene oxide; CNF: carbon nanofiber; SDS: sodium dodecyl sulfate; CNT: carbon nanotube; CPE: carbon paste electrode.

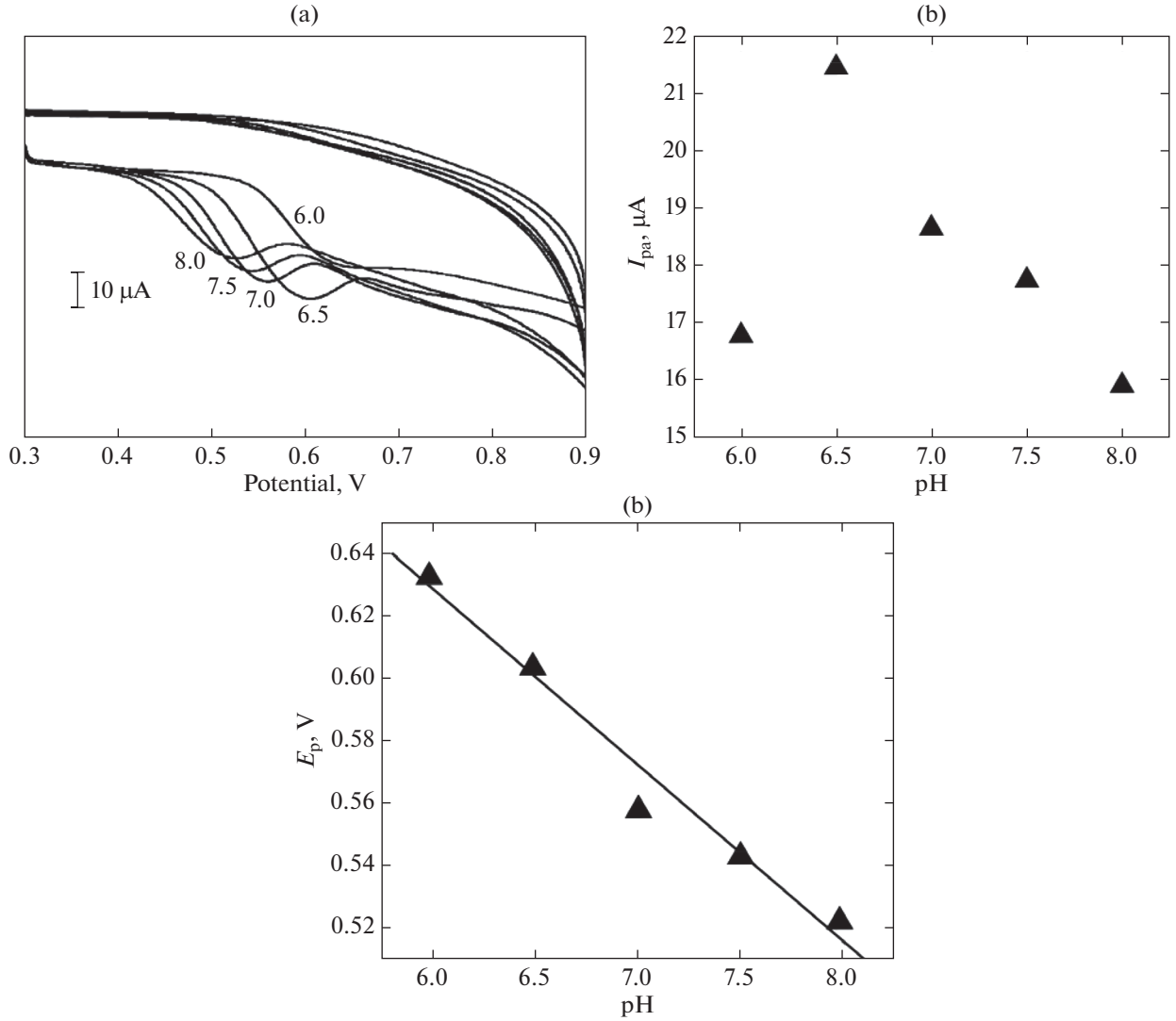

Fig. 7. (a) CVs of Tyr at solution pH 6.0–8.0; (b) dependence of anodic peak current (I_{pa}) of Tyr on solution pH; and (c) dependence of anodic peak potential (E_{pa}) of Tyr on solution pH.

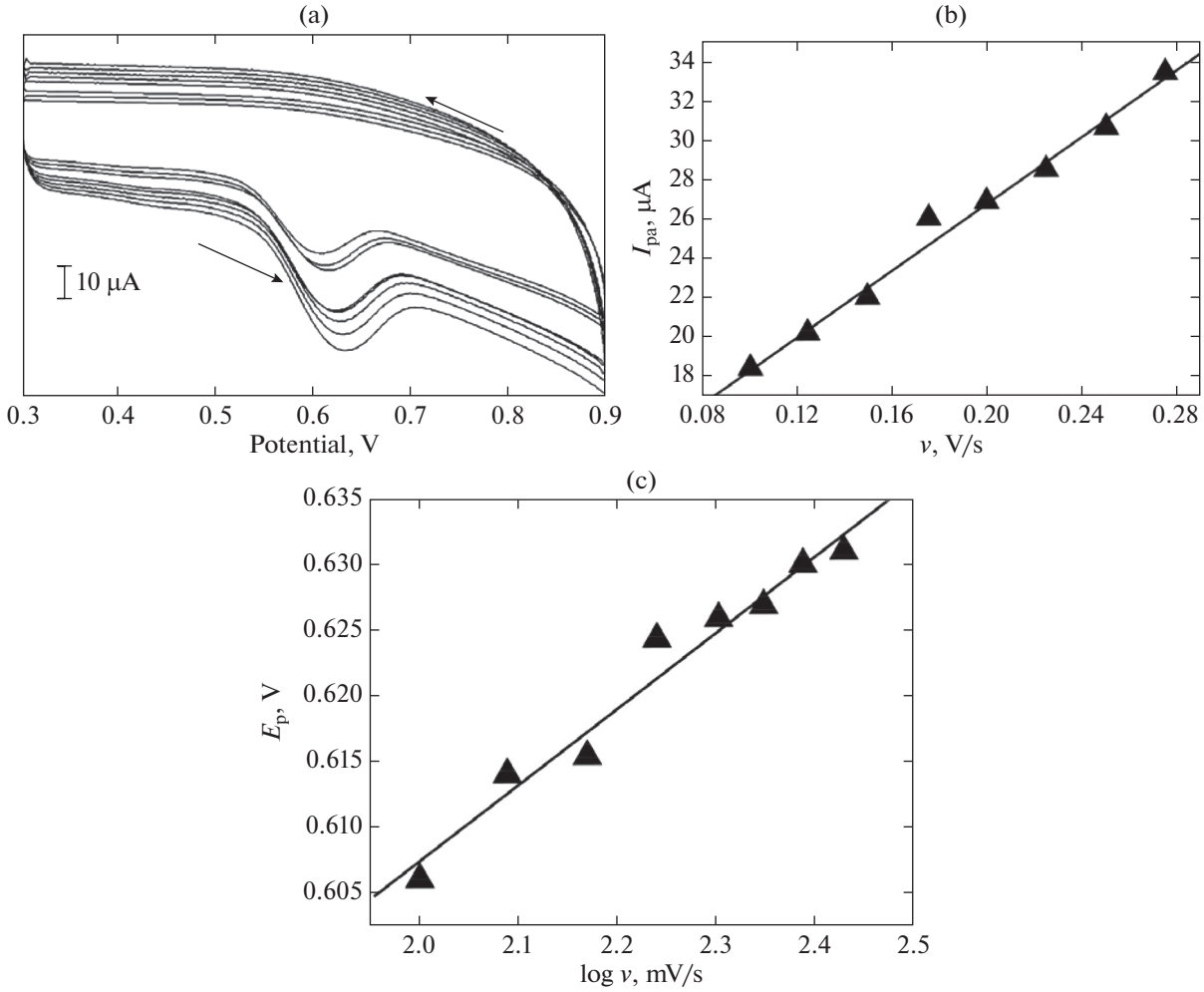

Fig. 8. (a) CVs of 1×10^{-4} M Tyr at PT/GCNT/PE, scan rate – 0.1–0.275 V/s; (b) plot of anodic peak current (I_{pa}) as function of scan rate; and, (c) plot of log of anodic peak current as function of peak potential.

of Tyr. It was observed that the peak current increased linearly with the Tyr concentration ranges of 2×10^{-6} to 2.5×10^{-5} M and of 3×10^{-5} to 1.2×10^{-4} M, with the corresponding linear equation: $I_{pa}(A) = 4.19 + 0.076$ M (C), with the correlation coefficient of 0.996 (Fig. 9). The limit of detection was estimated to be 2.9×10^{-7} M ($S/N = 3$), with S being the standard deviation for blank and N being the slope obtained from the calibration graph [44, 45]. Table 1 lists the comparison of some of the analytical parameters obtained for Tyr here with those published in [46–51].

Differential Pulse Voltammetry for Determination of Tyrosine

A differential pulse voltammetry (DPV) technique shows superior sensitivity and improved resolution in comparison with those via CV, as well as the background current which is negligible in DPV. DPV was performed in the concentration of Tyr 1×10^{-4} M. Figure 10 shows the DPV of Tyr at the bare (curve *a*) and modified (curve *b*) electrodes in 0.1 M PBS, pH 6.5, the scan rate 0.05 V/s, and the pulse width 0.05 Sec. The oxidation of Tyr at the bare electrode is at 0.643 V, with a low current response of 3.25 μA, but the current response at the modified electrode at the potential of 0.548 V was 11.70 μA which is 3.6 times higher than that obtained for the bare electrode. This can be associated with a strong electrocatalytic effect of the modified electrode in the direction of this compound.

Reproducibility and Stability of Modified Electrode

The reproducibility of PT/GCNT/PE was determined via 4 successive removals of the electrode. It was noticed that the relative standard deviation value of 3.1% for the analytes indicates that good reproducibility of the developed electrode. In addition, the stability of the modified electrode was measured by the current response decay during repetitive CV cycling

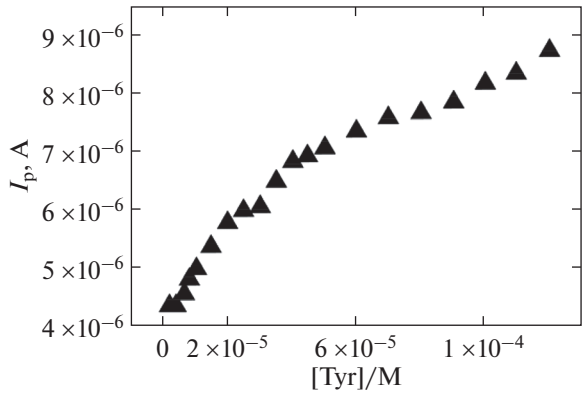

Fig. 9. Plot of oxidation peak current as function of Tyr concentration in 0.1 M PBS, pH 6.5 scan rate – 0.1 V/s.

(35) at room temperature in 0.1 M PBS, with pH 6.5 at the sweep rate of 0.1 V/s. It was found that there is a 9% decrease in the current from the initial value after 35 cycles, which demonstrates good stability of the electrode.

Electrochemical Investigations of Uric Acid and Ascorbic Acid

The UA shows a single voltammetric anodic peak with the peak current of I_{pa} = 13.23 μA and the peak potential E_{pa} = 0.261 V at the modified electrode at a sweep rate of 0.1 V/s in 0.1 M PBS (pH 6.5). Figure 11a shows the cyclic voltammogram of the modified (curve *a*) and the bare (curve *b*) electrodes. At the bare electrode, electrooxidation occurs at 0.254 V (1×10^{-4} M UA) in PBS buffer of pH 6.5, which proves slow electron transfer kinetics. It was observed that the oxidation of UA was irreversible. Figure 11b shows the cyclic voltammogram of UA at different scan rates. A linear relationship was obtained between the peak current and the scan rate with the linear regression equation of I_{pa} (μA) = 3.79 + 76.84 v (V/s) (Fig. 11c), with the correlation coefficient of 0.99.

The irreversible process on the electrode obeyed the following equation [52]

$$E_p(V) = E^0 + \frac{RT}{\alpha nF}\ln\frac{RTK_s}{\alpha nF} + \frac{RT}{\alpha nF}\ln v, \qquad (3)$$

where E^0 is the standard potential; R, T, F (ideal gas constant, temperature, faraday constant); K_s is the heterogeneous reaction rate constant; α is the charge transfer coefficient. From the slope of the E_{pa} vs ln$v$ plot, α value was obtained by equating the slope of $RT/\alpha nF$. For an irreversible process, α value is usually assumed to be 0.5. Herein, the electron transfer in the reaction was calculated to be 2.2~ = 2 and was theoretically close to 2.

The AA shows an anodic peak with the peak current of I_{pa} = 10.60 μA and the peak potential E_{pa} = –0.110 V at the modified electrode, at a sweep rate of 0.1 V/s in 0.1 M PBS, pH 6.5. Fig. 12a shows the cyclic voltammogram of the modified (curve *a*) and the bare (curve *b*) electrodes. At the bare electrode, no anodic peak was observed. It indicates that the electrocatalytic response is improved at the modified electrode. Fig. 12b presents the CVs of AA at the modified electrode with various scan rates. The oxidation peak shifted positively with a rise of the scan rate, which also shows a linear relationship of the scan rate with the regression equation of I_{pa} (μA) = 0.915 + 105.64v (V/s) with the correlation coefficient of 0.99. Figure 12c shows that the process on the modified electrode is an adsorption controlled one. The number of electrons transferred was calculated using the above equation. The slope of the graph E_{pa} vs ln$v$ was obtained to be 0.022, assuming the value of α is 0.5, the number of

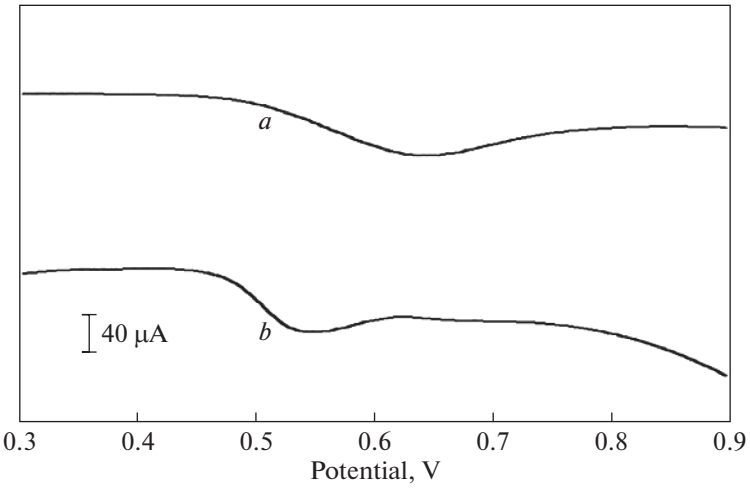

Fig. 10. Differential pulse voltammogram of 1×10^{-4} M Tyr at BGCNT/PE (curve *a*); and PT/GCNT/PE (curve *b*) in 0.1 M PBS, pH 6.5, scan rate – 0.05 V/s.

Table 2. Determination of Tyr in pharmaceutical samples

Sample	Added, mg	Found, mg	Recovery, %
1	0.4	0.396	99.00
2	0.48	0.488	101.85
3	0.56	0.575	102.8

electrons involved was calculated to be 2.3~ = 2, which is close to the theoretical value.

Simultaneous Determination of Tyrosine, Uric Acid, and Ascorbic Acid

To the best of the authors' knowledge, so far there is no research reported on the simultaneous resolution of Tyr, UA, and AA using PT/GCNT/PE. The most significant objective of the present was the simultaneous determination of Tyr, AA, and UA. This was performed using the CV technique. Figure 13 shows the cyclic voltammograms of Tyr (1×10^{-4} M), UA (1×10^{-4} M), and AA (1×10^{-3} M) in 0.1 M PBS, pH 6.5, with a scan rate of 0.1 V/s. Well-defined oxidation peaks of Tyr, AA, and UA were observed at 0.631 V, –0.0087 V, and 0.477 V, respectively, with the peak current responses of 26.20, 10.28, and 32.48 μA, respectively, representing that the simultaneous resolution of these electroactive species is achievable at PT/GCNT/PE.

Application of PT/GCNT/PE

A favourable electrochemical response of Tyr makes it a highly suitable object for the detection in pharmaceutical samples. To explain the applica-bility, a Tyr tablet was selected, and an analysis was accomplished by the standard addition method (Table 2). The recoveries obtained were from 99.00% to 102.80%, suggesting that the developed electrode is reliable and sensitive enough for the resolution of Tyr in real samples.

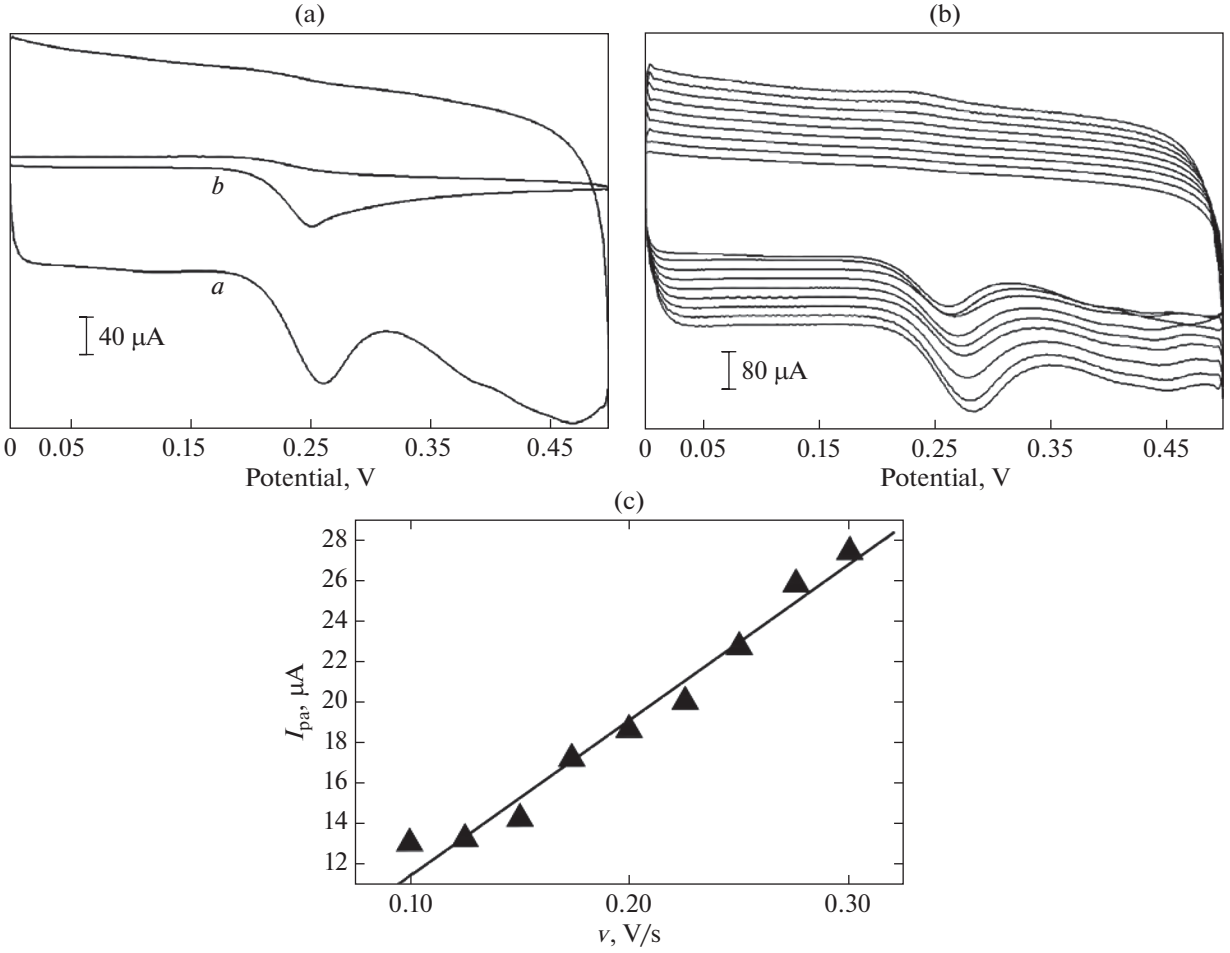

Fig. 11. (a) CVs of 1×10^{-4} M UA at PT/GCNT/PE (curve *a*) and BGCNT/PE (curve *b*) in 0.1 M PBS, pH 6.5 scan rate – 0.1 V/s; (b) CVs of 0.1 mM UA at PT/GCNT/PE at scan rate 0.1 – 0.300 V/s; and (c) plot of anodic peak current (I_{pa}) as function of scan rate.

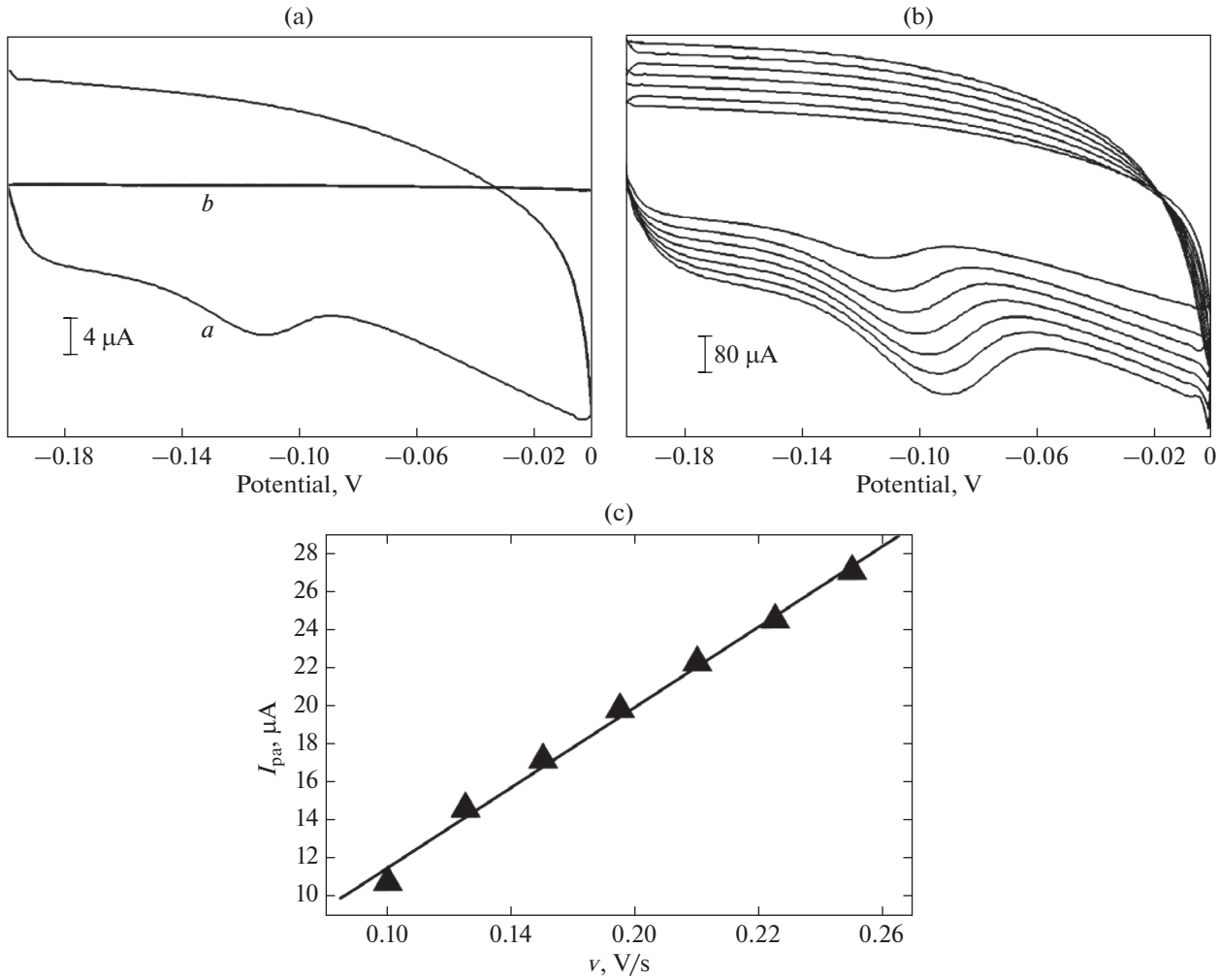

Fig. 12. (a) CVs of 1×10^{-3} M AA at PT/GCNT/PE (curve *a*) and BGCNT/PE (curve *b*) in 0.1 M PBS, pH 6.5, scan rate 0.1 V/s; (b) CVs of 1×10^{-3} M AA at PT/GCNT/PE, scan rate 0.1 – 0.250 V/s; (c) plot of anodic peak current (I_{pa}) as unction of scan rate.

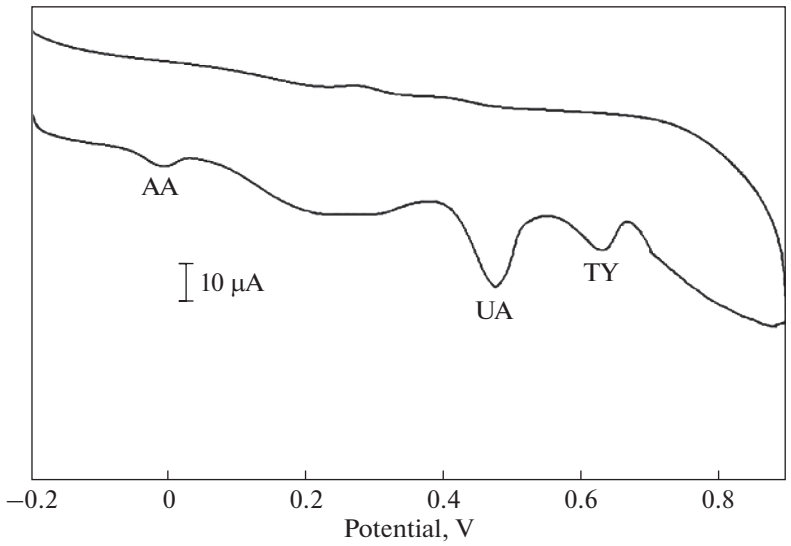

Fig. 13. CVs at PT/GCNT/PE, solution containing Tyr (1×10^{-4} M), UA (1×10^{-4} M), and AA (1×10^{-3} M) in 0.1 M PBS, pH 6.5.

CONCLUSIONS

In this study, a modified electrode (PT/GCNT/PE) was fabricated for the individual and concurrent resolution of Tyr, UA, and AA. Enhanced current responses were observed for these electroactive species at the modified electrode compared to those of the bare electrode. Under optimized conditions, the peak current of Tyr linearly was related to its concentration in a range of 2×10^{-6} to 2.5×10^{-5} M and of 3×10^{-5} to 1.2×10^{-4} M, leading to the detection limit of 2.9×10^{-7} M. The developed method could be applied to the resolution of Tyr in pharmaceutical sample with quite promising results. A high current response, a low limit of detection, and high selectivity of the modified electrode for the determination of Tyr demonstrate its potential as a sensor for practical use.

FUNDING

The authors gratefully acknowledge the financial support from the Vision Group on Science and Technology, Bangalore, India under the Research Project KSTePS/VGST-KFIST (L1) 2016-2017/GRD-559/2017-2018/126/333, 21/11/2017.

REFERENCES

1. Beck, G., Hanusch, C., Brinkkoetter, P., Rafat, N., et al., *Anaesthesist*, 2005, vol. 54, pp. 1012–1020.
2. Carlsson, A., Lindqvist, M., and Arch, N.S., *Pharmacology*, 1978, vol. 303, pp. 157–164.
3. Li, C.Y., *Colloids Surf., B*, 2006, vol. 50, pp. 147–151.
4. Cathcart, R.F., *Med. Hypotheses*, 1991, vol. 35, pp. 32–37.
5. Huang, Y., Jiang, X.Y., Wang, W., Duan, J.P., et al., *Talanta*, 2006, vol. 70, pp. 1157–1163.
6. Deng, C., Deng, Y., Wang, B., and Yang, X., *J. Chromatogr. B*, 2002, vol. 780, pp. 407–413.
7. Letellier, S., Garnier, J.P., Spy, J., and Bousquet, B., *J. Chromatogr. B*, 1997, vol. 696, pp. 9–17.
8. Yildiz, H.B., Freeman, R., Gill, R., and Willner, I., *Anal. Chem*., 2008, vol. 80, pp. 2811–2816.
9. Alonso, S., Zamora, L., and Calatayud, M., *Talanta*, 2003, vol. 60, pp. 369–376.
10. Manjunatha, J.G., *Asian J. Pharm. Clin. Res.*, 2017, vol. 10, pp. 295–300.
11. Sathish, R., Debasis, C., Shashanka, R., et al., *Anal. Bioanal. Electrochem*., 2013, vol. 5, pp. 455–466.
12. Manjunatha, J.G., Kumara, Swamy B.E., Mamatha, G.P., Raril, C., et al., *Mater. Today*, 2018, vol. 5, pp. 22368–22375.
13. Kumara Swamy B.E., Shashanka, R., and Debasis, C., *Int. J. Sci. Eng. Res.*, 2016, vol. 7, pp. 1275–1285.
14. Raril, C. and Manjunatha, J.G., *Anal. Bioanal. Electrochem*., 2018, vol. 10, pp. 372–382.
15. Shashanka, R., IntechOpen, . https://doi.org/10.5772/intechopen.80980
16. Manjunatha, J.G., *J. Surf. Sci. Technol.*, 2018, vol. 34, pp. 74–80.
17. Gururaj, K.J., Kumara, Swamy B.E., Norberto, C., and Flores-Moreno, R., *Electrochim. Acta*, 2017, vol. 258, pp. 1025–1034.
18. Manjunatha, J.G., *Sens. Biosens. Res.*, 2017, vol. 16, pp. 79–84.
19. Raril, C. and Manjunatha, J.G., *Anal. Bioanal. Electrochem*., 2018, vol. 10, pp. 488–498.
20. Manjunatha, J.G., *J. Food Drug Anal.*, 2018, vol. 26, pp. 292–299.
21. Manjunatha, J.G. and Deraman, M., *Anal. Bioanal. Electrochem*., 2017, vol. 9, pp. 198–213.
22. Gururaj, K.J. and Flores-Moreno, R., *Electrochim. Acta*, 2017, vol. 248, pp. 225–231.
23. Manjunatha, J.G., *J. Electrochem. Sci. Eng.*, 2017, vol. 7, pp. 39–49.
24. Manjunatha, J.G., Deraman M., Basri, N.H., and Talib, I.A., *Arab. J. Chem*., 2018, vol. 11, pp. 149–158.
25. Shashanka, R., Chaira, D., and Kumara Swamy, B.E., *Int. J. Electrochem. Sci*., 2015, vol. 10, pp. 5586–5598.
26. Manjunatha, J.G., *Int. J. ChemTech. Res*., 2016, vol. 9, pp. 136–146.
27. Raril, C. and Manjunatha, J.G., *Biomed. J. Sci. Tech. Res*., 2018, vol. 9, pp. 1–6.
28. Raril, C. and Manjunatha, J.G., *Modern Chem. Appl*., 2018, vol. 6, art. ID 1000263. https://doi.org/10.4172/2329-6798.1000263
29. Baghayeri, M., Veisi, H., Maleki, B., Karimi-Maleh, H., and Beitollahi, H., *RSC Adv*., 2014, vol. 4, pp. 49595–49604.
30. Shashanka, R., *Int. J. Sci. Eng. Res*., 2015, vol. 6, pp. 1863–1871.
31. Beitollahi, H., Hamzavi, M., Torkzadeh-Mahani, M., Shanesaz, M., et al., *Electroanalysis*, 2014, vol. 27, pp. 524–533.
32. Gururaj, K.J., Kumara Swamy, B.E., Chandrashekar, B.N., and Flores-Moreno, R., *J. Mol. Liq*., 2017, vol. 240, pp. 395–401.
33. Mohandoss, S. and Stalin, T., *Int. J. Adv. Res*., 2013, vol. 1, pp. 381–396.
34. Behpour, S.M., Jafari, M.N., and Khoobi, A., *Anal. Lett*., 2013, vol. 46, pp. 299–311.
35. Beitollahi, H., Nekooei, S., and Torkzadeh- Mahani, M., *Talanta*, 2018, vol. 188, pp. 701–707.
36. Gururaj, K.J., Kumara Swamy, B.E., Ramirez, H.N.G., Ekanthappa M.T., et al., *New J. Chem*., 2018, vol. 42, pp. 4501–4506.
37. Kemula, W. and Kublik, Z., *Nature*, 1958, vol. 182, pp. 793–794.
38. Wang, L., Huang, P., Bai, J., Wang, H., et al., *Int. J. Electrochem. Sci*., 2006, vol. 1, pp. 334–342.
39. Wang, S., Xu, Q., and Liu, G., *Electroanalysis*, 2008, vol. 20, pp. 1116–1120.
40. Islamnezhada, A. and Jobaneh, E.F., *Adv. Mater. Res*., 2013, vol. 829, pp. 675–680.
41. Filik, H., Avan, A.A., and Aydar, S., *Arab. J. Chem*., 2016, vol. 9, pp. 471–480.
42. Arvand, M., Pourhabib, A., and Giahi, M., *J. Pharm. Anal*., 2017, vol. 7, pp. 110–117.
43. Jiang, L., Shuqing, G., Ding, Y., Daixin, Y., et al., *Colloids Surf., B*, 2013, vol. 107, pp. 146–151.

44. Raril, C., Manjunatha, J.G., Nanjundaswamy, L., Siddaraju, G., et al., *Anal. Bioanal. Electrochem.*, 2018, vol. 10, pp. 1479–1490.
45. Ya, Y., Luo, D., Zhan, G., and Chunya, L., *Bull. Korean Chem. Soc.*, 2008, vol. 29, pp. 928–932.
46. Behpour, M., Masoum, S., and Meshki, M., *J. Nanostruct.*, 2013, vol. 3, pp. 243–251.
47. Denga, K.Q., Zhou, J.H., and Li, X.F., *Colloids Surf., B*, 2013, vol. 101, pp. 183–188.
48. Tang, X., Liu, Y., Hou, H., and You, T., *Talanta*, 2010, vol. 80, pp. 2182–2186.
49. Hareesha, N., Manjunatha, J.G., Raril, C., and Girish, T., *Adv. Pharm. Bull.*, 2019, vol. 9, pp. 132–137.
50. Ghoreishi, S.M., Behpour, M., Delshad, M., and Khoobi, A., *Central Eur. J. Chem.*, 2012, vol. 10, pp. 1824–1829.
51. Chitravathi, S., Kumara Swamy, B.E., Mamatha, G.P., and Chandrashekar, B.N., *J. Mol. Liq.*, 2012, vol. 172, pp. 130–135.
52. Raril, C. and Manjunatha, J.G., *Curr. Top. Electrochem.*, 2019, vol. 21, pp. 93–105.

SPELL: 1. OK